



Transparent, Pliable, Antimicrobial Hydrogels for Ocular Wound Dressings

Tao Liu ¹, Eleonore C.L. Bolle ¹, Traian V. Chirila ^{2,3,4,5,6} , Marion Buck ⁷, Daniel Jonas ⁷, Shuko Suzuki ², Tai Smith ^{2,3}, V. Prasad Shastri ^{8,9}, Tim R. Dargaville ^{1,2} and Aurelien Forget ^{1,2,9,*} 

- ¹ Institute of Health and Biomedical Innovation, Faculty of Science and Engineering, Queensland University of Technology, Brisbane, QLD 4001, Australia; t24.liu@connect.qut.edu.au (T.L.); e.bolle@qut.edu.au (E.C.L.B.); t.dargaville@qut.edu.au (T.R.D.)
- ² Queensland Eye Institute, 140 Melbourne Street, South Brisbane, QLD 4101, Australia; traian.chirila@qei.org.au (T.V.C.); shuko.suzuki@qei.org.au (S.S.); taismith@optusnet.com.au (T.S.)
- ³ Faculty of Science and Engineering, Queensland University of Technology, Brisbane, QLD 4001, Australia
- ⁴ Australian Institute of Bioengineering & Nanotechnology, University of Queensland, St Lucia, QLD 4072, Australia
- ⁵ Faculty of Medicine, University of Queensland, Herston, QLD 4029, Australia
- ⁶ Faculty of Sciences, University of Western Australia, Crawley, WA 6009, Australia
- ⁷ Institute for Infection Prevention and Hospital Hygiene, University Hospital, 79104 Freiburg, Germany; marion.buck@uniklinik-freiburg.de (M.B.); daniel.jonas@uniklinik-freiburg.de (D.J.)
- ⁸ BIOS Centre for Biological Signaling Studies, University of Freiburg, 79104 Freiburg, Germany; prasad.shastri@makro.uni-freiburg.de
- ⁹ Institute for Macromolecular Chemistry, University of Freiburg, 79104 Freiburg, Germany
- * Correspondence: aurelien.forget@makro.uni-freiburg.de

Received: 30 September 2020; Accepted: 23 October 2020; Published: 27 October 2020



Abstract: Following ocular surgery, dressings are commonly applied to the surgical wound. These dressings need to combine medical properties with ease of use while maintaining comfort for the patient. For the ocular area, this means that the dressings need to act as a microbial barrier, allow good conformability to the contours of the eye, and provide evaporative cooling to the inflamed area. Furthermore, the dressings should be transparent to allow for the inspection of the wound site by healthcare professionals without the need for removal. In this paper, we investigate a blend of native agarose (NA) and carboxylated agarose (CA) for producing elastic hydrogels with high water content that can be supplemented with antibiotics. It was found that in comparison to pure agarose hydrogels, the NA hydrogels blended with CA had a reduced Young's modulus, reduced evaporation rate when exposed to air, and accelerated release rate of antimicrobial agents, whilst maintaining the same degree of transparency. By altering the formulation from 2 wt.% pure NA to 1 wt.% NA blended with 1 wt.% CA, we were able to observe an approximately 55% reduction in Young's modulus, 25% reduction in evaporation rate, as well as a significant acceleration in the release rate of cefazolin and doxycycline, making this hydrogel blend a potential material for topical treatment applications.

Keywords: hydrogel; wound dressing; antimicrobial

1. Introduction

Surgical procedures on the eye or its surrounding such as oculoplastic or extraocular muscle surgeries are followed up by the application of a wound dressing. Several types of dressings can be used, but transparent ones have the advantage of allowing for wound osculation without removing the dressing while providing non-obstructed vision for the patient [1]. Current clinical practices use dressings composed of agar and polyacrylamide polymer [2], cotton gauges to deliver pharmaceuticals to the eye [3], and polyurethane-based drug eluting dressings [4]. Hydrogel dressings, because of

their high content of water, produce a cooling effect on the wound, helping to reduce the warm feeling associated with inflammatory tissues [5]. Often, in addition to the dressing, the wound care is accompanied by the application of antibiotics, which can help reduce wound infection and support wound closure [6]. However, for a transparent wound dressing that releases an antimicrobial molecule to be adequate for ocular wounds, it needs to be pliable to follow the intricate eye anatomy, yet mechanically robust to remain in place for a long period [7].

In recent years, the possibility of manufacturing high-performance and multi-purpose wound dressings with non-woven materials has been widely explored. Such materials include chitosan [8–10], alginate [11,12], and bacterial cellulose [13]. Due to the range of unique properties, agarose, a polysaccharide sourced from seaweed, has found uses in biomedical [14], cosmeceutical [15], and food applications [16]. One of the most useful properties of agarose is its capability to form physically crosslinked hydrogels that are biocompatible and inert [17]. Agarose hydrogels exhibit hysteresis in their phase behavior, that is, they are soluble at temperatures above 90 °C while they form a gel below 40 °C [18].

Blending can be used as a technique to manipulate hydrogel properties for various applications. Successful examples of this include hydrogel blends of agarose–methylcellulose for the control of the gelation time and temperature [19], agar–poly(vinyl alcohol) for control of the mechanical properties [20], and gelatine–hydroxyethyl cellulose for control over drug release rate [21].

Agarose can be chemically modified through a controlled carboxylation of the polysaccharide backbone (Figure 1A) to obtain carboxylated agarose (CA) and gain precise control over the mechanical properties of the modified hydrogel by inducing a switch of the secondary structure from α -helical to β -sheet [22]. Blending native agarose (NA) with different amounts of CA, leads to gels with predictable shear moduli ranging from 0.1 to 100 kPa [23].

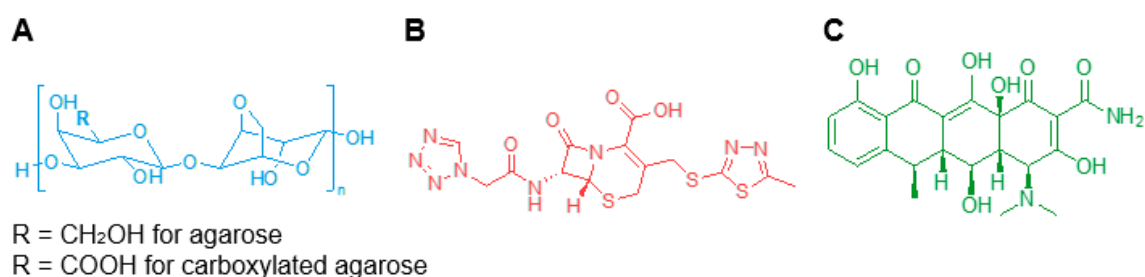


Figure 1. Chemical structures of (A) native and carboxylated agarose, (B) cefazolin, and (C) doxycycline.

While blending offers considerable industrial advantage for the industrial manufacturing of hydrogels with broad mechanical properties, neither NA nor CA possess intrinsic anti-microbial properties. However, based on their good molecular transport properties [24], here, we attempted to exploit NA–CA hydrogel blends to formulate wound dressings capable of carrying antimicrobial agents and providing continuous topical drug delivery for over ten hours.

In this study, we investigated three hydrogel blends using a total solids content of 2 wt.% consisting of NA-to-CA ratios ranging from 100% to 50%: NA100, NA75CA25, and NA50CA50. The hydrogel blends were formulated with the two different antimicrobial molecules, cefazolin and doxycycline (Figure 1B,C), and their transparency, water evaporation, mechanical properties, and drug release capabilities were characterized *in vitro*. The biological properties of the formulated hydrogels were then tested against two common bacteria strains, *Escherichia coli* and *Staphylococcus aureus*, associated with eye infections.

2. Materials and Methods

2.1. Materials

Native agarose with a low melting temperature from ThermoFisher Scientific (Scoresby, Australia) was used as received. Carboxylated agarose (degree of carboxylation = 93%) was received from the Institute for Macromolecular Chemistry, University of Freiburg in Germany and was stored at 4 °C. Cefazolin sodium salt (AFT Pharmaceuticals, North Ryde, Australia) and doxycycline (Sigma-Aldrich, North Ryde, Australia) were used as received. Phosphate-buffered saline (PBS) was from ThermoFisher Scientific (Scoresby, Australia) and *Staphylococcus aureus* (ATCC 29213) and *Escherichia coli* (ATCC 25922) were obtained from ATCC (Wesel, Germany).

2.2. Hydrogel Pads

NA and CA (93% carboxylation) were combined in the desired ratios and solubilized in PBS by heating in a microwave oven until complete solubilization of the polysaccharides was achieved [14]. The concentration of total polysaccharides (NA and CA) in PBS was 2% w/v for all formulations. The hydrogel-forming hot solutions were slowly cooled to 60 °C in warm water, and antimicrobial agents, if any, were then mixed with the solutions and homogenized by vortex mixing. The hot solutions were then cast in molds (details below) and cooled at 4 °C. A hydrogel fitting on a human was performed on the corresponding author, and pictures were acquired with a digital camera (iPhone 8, Apple).

2.3. Measurement of Absorbance

Hot solutions of hydrogel were poured into a 1 mL cuvette ($n = 3$). For each sample, the UV-visible spectra were recorded between 250 and 700 nm on a spectrophotometer (Nanodrop, ThermoFischer).

2.4. Measurement of Water Evaporation Rates

Hot hydrogel-forming solution (3 mL) was transferred into 15 mm diameter glass petri to form hydrogel samples of approximately 3 mm thickness ($n = 5$). Each sample was weighed every 10 min over 12 h on a GR202 digital scale (A&D Weighing, Tokyo, Japan) attached to a computer. The hourly evaporation rates were calculated based on scaled averages and normalized to the surface area exposed to air.

2.5. Tensile Testing

Hot hydrogel-forming solutions (10 mL) were transferred into dog-bone shaped PMMA molds that were custom made by laser cutting (geometries in compliance with ISO527-2 Type 1A, Figure S1), followed by refrigeration at 4 °C for 15 min to allow for complete gelation. The multilayer design of the molds allowed the gauze pieces to be integrated with hydrogel samples at the end sections during the gelation process. An Instron 5943 testing machine (Instron, Norwood, MA, USA) and Bluehill 3 console software was used to characterize tensile properties. Pneumatic grips were applied on gauze pieces instead of directly on the hydrogel to avoid alteration of the samples. The experiment was carried out at room temperature at a strain rate of 1 mm/min for 2 min to equilibrate the samples followed by an increase in the strain rate to 20 mm/min to generate the stress–strain curve in compliance with ISO 527 ($n = 3$).

2.6. Hydrogel Swelling

Each formulation was dissolved in deionized water and 2 mL was casted in a 6-well plate. The hot solution was cooled down at 4 °C to form a gel. Then, disks of 6 mm in diameter were punched out with a biopsy punch. Each disk was weighed and loaded in a 24-well plate. Three samples per time point per formulation were prepared. At each time point the disks were blotted and weighed.

The percentage of swelling was measured as the difference between the swollen mass and the dry mass divided by the dry mass.

2.7. Release of Antimicrobials

Hydrogel-forming solutions (100 μ L) loaded with antimicrobials (1 mg/mL) were pipetted into each well ($n = 5$) of a 96-well glass plate and cooled at 4 $^{\circ}$ C to form the hydrogel samples. Once the gelation was complete, 100 μ L of PBS solution was pipetted into each well to allow for the diffusion of antimicrobials out of the hydrogels. The PBS solutions were replaced after 5 min of release and transferred into empty wells. The replacement of PBS solution was then repeated at 10 min, 15 min, 30 min, 1 h, 2 h, 4 h, and 12 h. The PBS solutions were analyzed with an AD200C Plate Reader (Beckman Coulter, Australia) to determine the concentration of antimicrobials via measurement of absorbance. Calibration curves to link absorbance to the concentration were performed prior to this experiment (Figure S2). For both cefazolin and doxycycline, the absorbance was measured at $\lambda = 271$ nm. The antibiotic release was taken as the total accumulated release.

2.8. Antimicrobial Activity

The minimum inhibition concentration (MIC) was determined using the Mueller-Hinton (MH) broth micro-dilution methodology. Briefly, cefazolin and doxycycline (1.024 mg/mL in PBS) was serially diluted in a 50 μ L volume of MH broth in a 96-well plate starting from a concentration of 512 μ g/mL up to 3.7 ng/mL. Following this, bacteria were introduced in a 50 μ L volume into each well. Overnight culture of the bacterial strains on blood agar was used to inoculate the MH broth to reach an absorbance of 0.08 and 0.12 for *S. aureus* and *E. coli*, respectively. The inoculum was then diluted 1:100 before being introduced into each well. The negative controls contained only 100 μ L MH broth, while 100 μ L MH broth containing bacteria served as a positive control. Plates were incubated for 24 h at 36 $^{\circ}$ C, and the MIC was determined as the concentration of antimicrobial molecules in the well that did not allow any bacterial colony formation. MIC was determined by three independent experiments with duplicate runs each time. Colony forming units (CFU)/mL for each bacterial inoculum were calculated following spread plating of 10 μ L of 1:100 dilution of the bacterial inoculum (used for MIC studies) on blood agar plates. The end concentration of the bacterial inoculum was maintained in the range of 5×10^4 to 7×10^5 CFU/mL.

Zone of inhibition (ZOI) was measured using the following protocol. Hydrogels loaded with cefazolin or doxycycline were punched into discs of 9 mm diameter. As mentioned in the MIC study, *S. aureus* and *E. coli* were cultured in MH broth to reach an absorbance of 0.09 and 0.14, respectively. They were then spread end-to-end on MH agar plates using a cotton swab in three different directions. Following this, the hydrogel disks containing the antimicrobial and 2% w/v polysaccharide were positioned on the agar plates and incubated for 24 h at 36 $^{\circ}$ C. A similar set up was used for the control disks. The ZOI was measured as the distance from the disc where no bacterial growth was observed.

3. Results

3.1. Transparency of Blended Hydrogel is Independent of Formulation

In the agarose networks, the opacity originates from the scattering of light by the crosslinking points [25]. Therefore, differences in the density, shape, and size of the crosslinking points will affect the opacity of the resulting hydrogel network. Based on our previous work, we hypothesized that by reducing the crosslinking density via the introduction of CA, the transparency of the hydrogel blend could be enhanced [26]. We observed similar absorbance patterns in NA and NA75CA25 samples. However, in the 1:1 NA-to-CA ratio (NA50CA50) a lower absorbance in the red wavelength was observed (Figure 2A). This translated into a hydrogel that was more transparent than the other dressings formulated with a higher content of NA (Figure 2B). This suggests that increasing the proportion of CA, increased the transparency of the hydrogel and that the NA50CA50 formulation is better suited for

the manufacturing of transparent wound dressings. It should be noted that above ~60% CA content, the crosslinking between polysaccharide chains was weakened to a point where the hydrogel could not maintain a rigid shape under its own weight when handled and therefore >50% CA content was not considered.

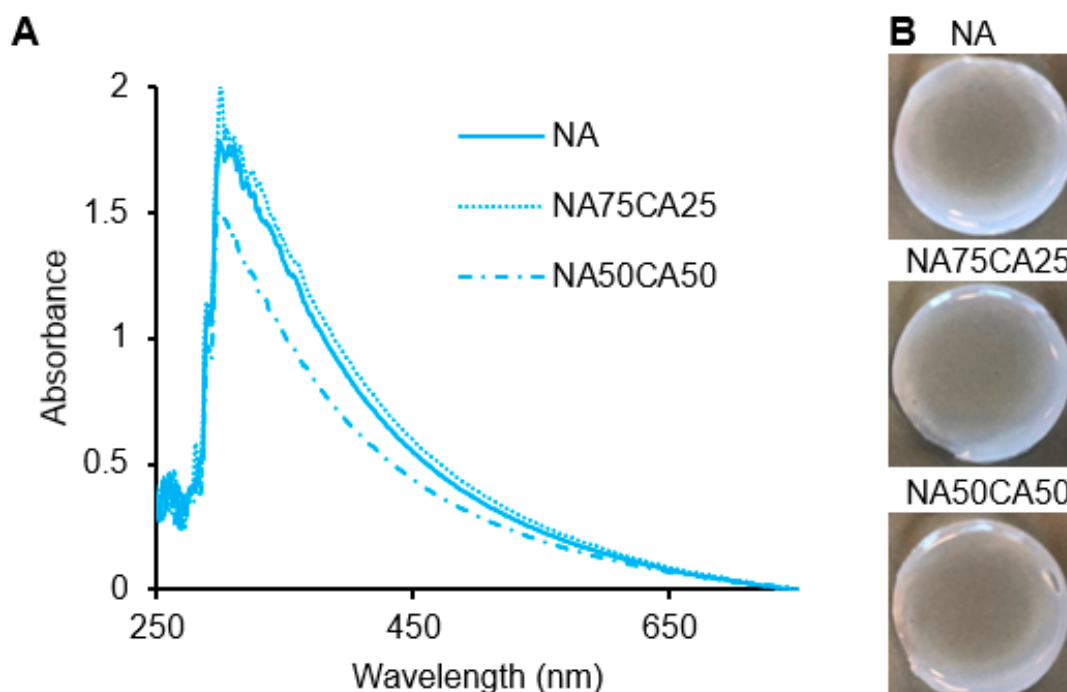


Figure 2. (A) UV-visible spectra of the three formulations showing a higher transparency in the NA50CA50 sample. (B) Photography of the hydrogel pad showing the opacity of each formulation. NA: native agarose; CA: carboxylated agarose.

3.2. Carboxylated Agarose Retards Water Evaporation from Hydrogels

Wounds are associated with an inflammatory response from the body, which can cause a warm sensation. Hydrogels, due to their high-water content, are particularly well suited to provide a local cooling effect due to the high heat capacity of water. Since water evaporation is an endothermic phenomenon, as the water evaporates, the area under the hydrogel is cooled down, leading to a cooling sensation. To assess the potential cooling effect of the hydrogel, we measured the evaporation rate of water of the three hydrogel formulations (NA, NA75CA25, and NA50CA50) by measuring the weight loss over 12 h at 50% humidity. Results indicated that increasing the concentration of CA in the hydrogel formulation resulted in a slower evaporation rate (Figure 3). By replacing 50 wt.% of NA with CA in the polysaccharide composition, we observed a 24.6% drop in the rate of evaporation in 3 mm thick gel samples. The NA samples showed an evaporation rate of 10.0, the NA75CA25 of 9.2, and the NA50CA50 of 7.5 mg/cm²/hour. This change in evaporation rate could originate from the increased number of potential hydrogen bonds in the CA hydrogel through the introduction of carboxylic acid functional groups. The carboxylic acid functional groups could form hydrogen bonds with the surrounding free water, thus reducing the evaporation rate [27]. While a higher cooling rate is favorable to provide a higher cooling effect, a slower evaporation could maintain the cooling effect for a longer time. For a wound dressing application, a prolonged cooling effect could be beneficial to extend the use of the dressing.

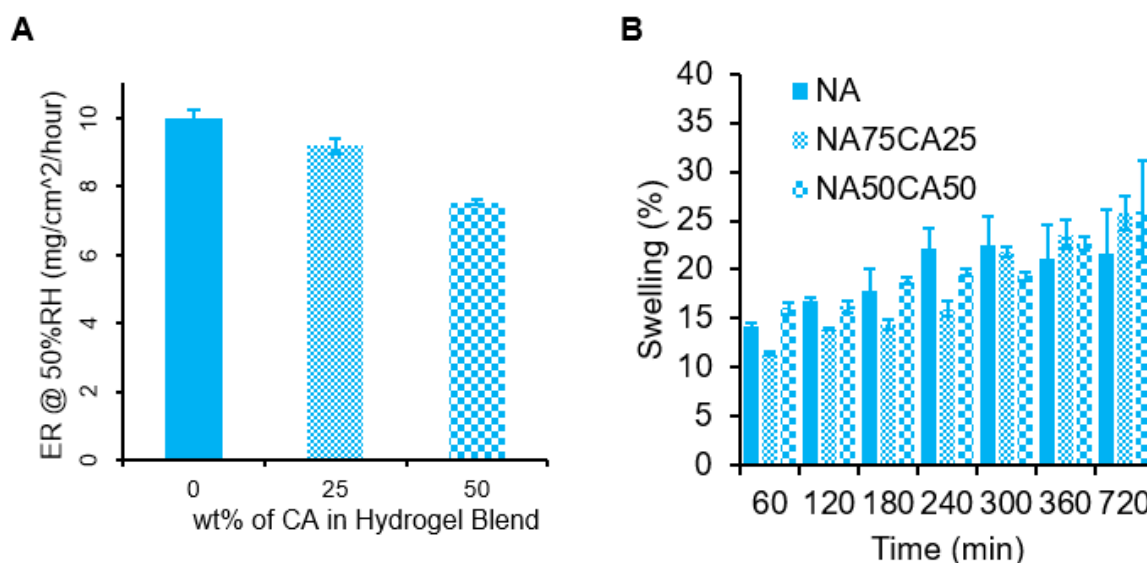


Figure 3. (A) Rate of water evaporation (ER) from 3 mm thick hydrogel blends for 12 h at 50% humidity, with measurements taken every 10 min. The results are normalized and have units of mg/cm²/hour. Error bars show standard error for $n = 5$. (B) Hydrogel swelling for each formulation measured over 12 h.

Applied to post-surgical wounds, the water evaporation phenomenon might be affected by the swelling behavior of the hydrogel in contact with physiological fluids such as sweat or wound exudate. Therefore, the swelling capacity of the three formulations were measured over 12 h (Figure 3B). NA showed the highest swelling capacity at the beginning of the experiment. The NA hydrogels were saturated at 300 min. After 300 min, it was found that the CA blended hydrogels swelled slowly to a final mass increase of 26% \pm 5% for the NA50CA50 formulation. Increasing the proportion of carboxylated agarose in the formulation results in an increase in swelling capacity after 300 min. An increased swelling capacity may be beneficial for exuding wounds, as it can be expected that hydrogels with an increased swelling capacity can absorb a higher amount of wound exudate, thus helping to keep the wound clean.

3.3. Elastic Modulus and Swelling Behavior of Blended Hydrogels are Dependent on the Content of Carboxylated Agarose

The elasticity of the hydrogel blends was characterized by measuring the Young's modulus in elongation. The stress–strain curves (Figure S3) showed that all samples exhibit linear elasticity with minimal plastic deformation prior to break. This suggests that the failure mode of the NA–CA hydrogel blend in elongation is a fast fracture propagation with a negligible post-yield-stress region. Furthermore, we found, as illustrated in Figure 4A, that the Young's moduli of the hydrogel blends dropped linearly as the percentage of CA content increased. When the introduction of CA was increased to 50% of total polysaccharides, a 55% decrease in the material's Young's modulus was observed, making the blended hydrogel twice as elastic as the pure agarose hydrogel (Figure 4A).

It has been suggested by Arnott et al. [18] that the mechanical properties of agarose hydrogels are dominated by the gel's interaction between the α -helix secondary structures of the polysaccharide chains leading to closely-knitted crosslinks between polysaccharide chains to form and assemble into a network. However, introduction of the carboxylic acid group in the agarose polymer backbone induces a switch in the secondary structure from an α -helix to a β -sheet structure [14,22]. This switch induces a disruption of the crosslinking points. We have previously demonstrated that this disruption of crosslinking points can also be achieved by blending NA with CA, inducing a lower shear modulus of the hydrogel [26]. Here, we showed that the introduction of CA into the NA matrix induced a decrease of the elastic modulus.

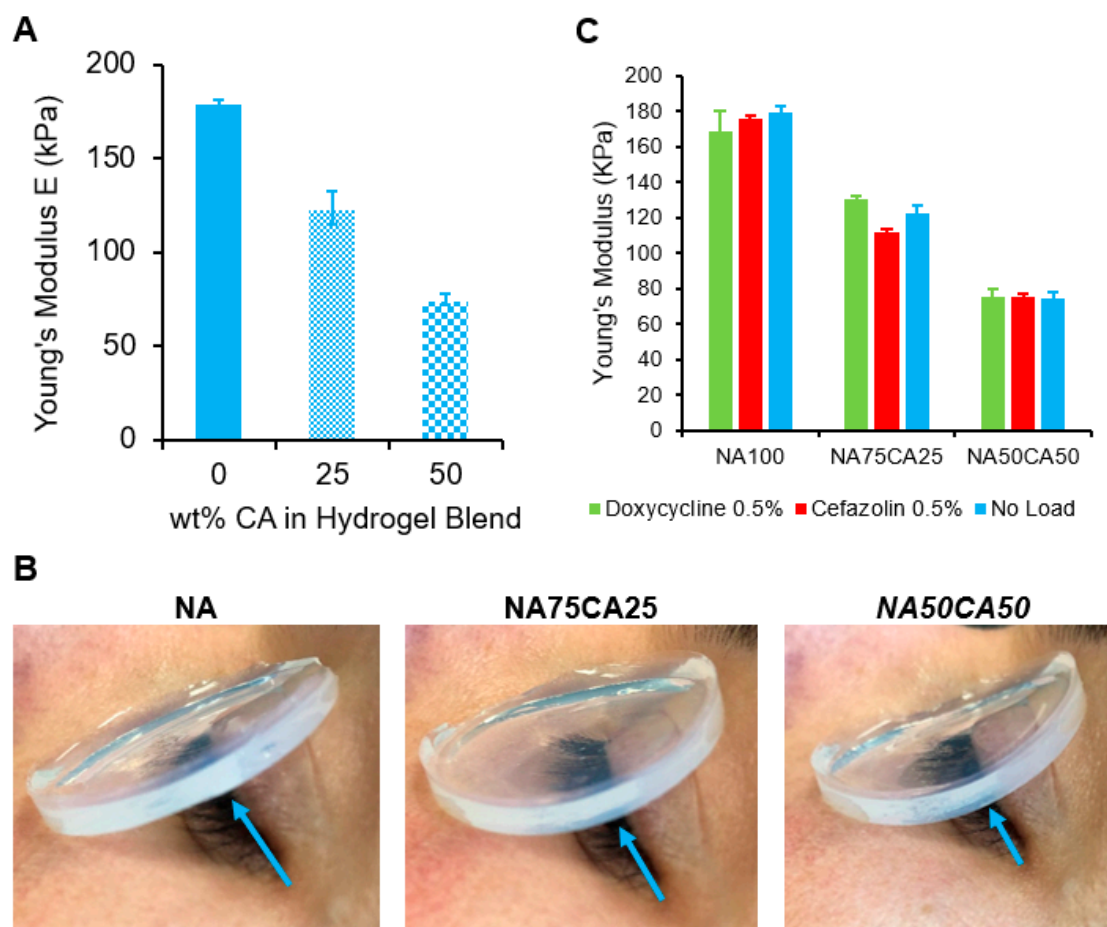


Figure 4. (A) Plot of Young's moduli versus wt.% of CA in total weight of polysaccharide. A near-linear relationship can be observed. (B) Young's moduli of hydrogel blends loaded with cefazolin and doxycycline, respectively, compared with antimicrobial-free blends (blank hydrogels). Suggesting that a 0.5% load of antimicrobial agents does not affect the modulus of an NA–CA hydrogel. (C) Flexibility of the hydrogel pads assessed on a human eye. Blue arrow shows the increased curvature of the hydrogel as the concentration of CA increases.

For ocular wound dressing applications, low elastic modulus is desirable, as a flexible dressing can better follow the contours of the eye and eye-socket to ensure contact between the dressing and the wound. In this regard, the blend with the highest concentration of CA (NA50CA50) is preferred (Figure 4B).

After ocular surgery, eye infection can lead to tremendous complications and longer hospitalization. Therefore, wound dressing that would release an antimicrobial molecule could help to reduce post-operative infections. As the mechanical properties of the NA/CA hydrogel blend are heavily influenced by the polysaccharide network structure, we tested if the loading of antimicrobial molecules in the hydrogel may affect the hydrogel's mechanical properties. We measured the elastic modulus of each formulation containing 3 mg/mL of the two selected antimicrobials (cefazolin and doxycycline). We observed that the antimicrobials did not induce a variation of the Young's modulus. This is likely due to the concentration of antimicrobials that is too low to have an impact on the hydrogel network formation (Figure 4C).

3.4. Carboxylated Agarose Allows Control Over Release Profile of Antimicrobial Agents

The cumulative release profiles of cefazolin and doxycycline from hydrogel samples into a PBS solution was measured over the course of 12 h (Figure 5A,B). For both antimicrobials, the introduction

of CA increased the release rate. The addition of 50% of CA in the formulation NA50CA50, led to an 81% total release of cefazolin within the first 6 h. The release after 12 h was complete only in the hydrogels formulated with CA. For the doxycycline, the release was slower and after 12 h only 80% of the drug was released in the NA50CA50 formulation. Nevertheless, the effect of CA on acceleration of diffusion of antimicrobial molecules from hydrogel samples into PBS is here clearly demonstrated.

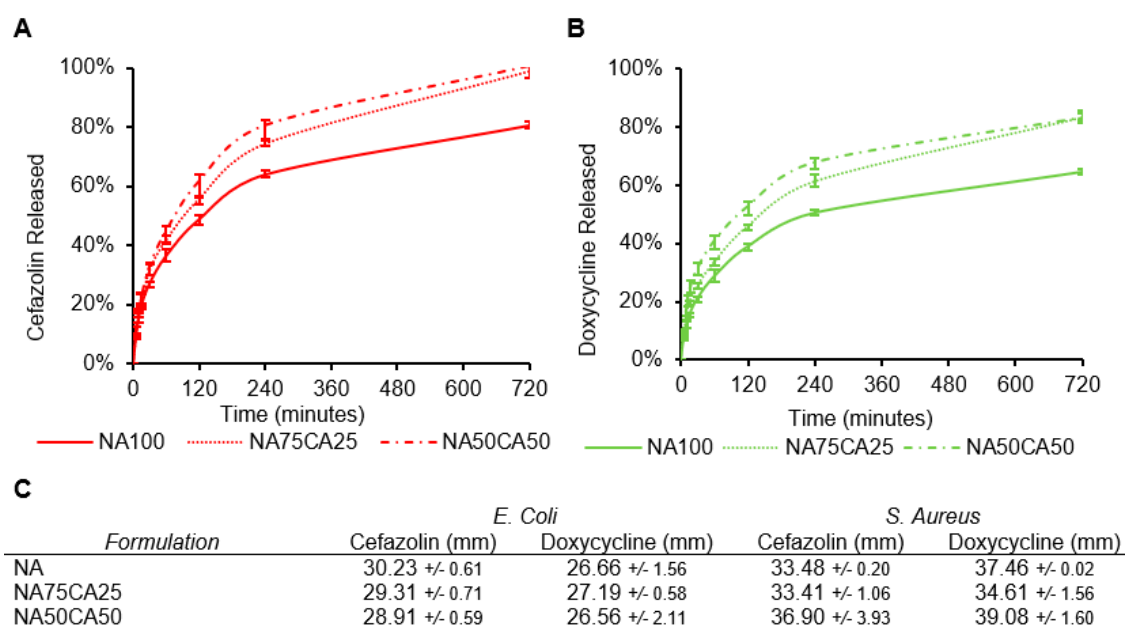


Figure 5. Release profiles of (A) cefazolin and (B) doxycycline in phosphate-buffered saline (PBS). The effect of CA on the acceleration of the release rate is apparent for the two types of antimicrobial agents tested. (C) Zone of inhibition of the three hydrogel formulations each loaded with 3 mg/mL of antimicrobial and tested on *Escherichia coli* and *Staphylococcus aureus*. (N = 3, standard deviation).

While the two antimicrobials are water soluble, at pH 7.4, most carboxylic acid groups on cefazolin will be deprotonated resulting in an overall negative charge. Conversely, doxycycline will be in the zwitterion and might interact with the negative charges of the CA [28]. When compared with doxycycline, the negative charge on cefazolin could explain the faster release from the negatively charged CA network. Electrostatic repulsions between the charged polysaccharide network and the charged molecule could influence the release rate. For the application of these hydrogel blends as a wound dressing, a continuous antimicrobial activity during the application window is desirable.

As a wound dressing, the hydrogel devices form a barrier to prevent infection. Additionally, hydrogels due to their aqueous environment are an ideal environment for bacterial growth. Supplementing the CA/NA blends with antimicrobial agents offers the possibility to avoid bacteria growth in the hydrogel but also around the hydrogel as the antimicrobial agent diffuses outside. First, the minimum inhibitory concentration (MIC) for the antimicrobial molecules was determined against Gram negative (*E. coli*) and Gram positive (*S. aureus*) strains. The MICs for cefazolin and doxycycline against *E. coli* were 2 μ g/mL and 0.25 μ g/mL, respectively. Similarly, for *S. aureus* the MIC was 0.5 μ g/mL for cefazolin and 0.25 μ g/mL for doxycycline.

To characterize the efficacy of the blend formulations we performed a zone of inhibition (ZOI) assay. Each of the antimicrobials was loaded in the different hydrogel formulations and the potency of the different formulation was evaluated. As expected from the MIC and release kinetics, cefazolin and doxycycline lead to a broad ZOI and both antimicrobials are more efficient against *S. aureus* than *E. coli*. While in the release experiment, we observed slight differences in the release rates of the antimicrobials across the different formulations, on both strains we obtained a similar ZOI across the three formulations. All three formulations resulted in similar ZOI against both strains. The ZOI

against *E. coli* ranged between 28.2 and 30.2 mm for cefazolin and between 26.5 and 27.6 mm for doxycycline. ZOI against *S. aureus* ranged between 33.4 and 36.9 mm for cefazolin and 34.6 and 39.1 mm for doxycycline (Figure 5C). Together, the ZOI results confirmed that both antibiotics retain their biological activity when released from the hydrogel formulations, and that the addition of CA did not alter the ZOI over 24 h.

4. Discussion

This study proposes the use of chemically modified marine polysaccharides as a transparent, flexible, drug-eluting wound dressing. Through simple blending of native agarose (NA) with its chemically modified counterpart, carboxylated agarose (CA), we obtained a material candidate for topical antimicrobial delivery applications. Via the introduction of CA in the blend, the flexibility and elasticity of the resulting wound dressing prototype was significantly improved. Furthermore, the rate of water evaporation was decreased, and the release rate of anti-microbial agents including cefazolin and doxycycline was accelerated. From the three different formulations studied, the hydrogel blend with 50% CA content (NA50CA50) exhibited the most optimal properties for imparting a cooling effect, transparency, and rapid release of antimicrobial agent. The blending approach provides a considerable advantage in terms of translation and manufacturing opportunity by allowing the precise tuning of key features of the wound dressing by simple mixing of two components. This approach could be used for the engineering of classes of wound dressings, each designed for a different application.

Supplementary Materials: The following are available online at <http://www.mdpi.com/2076-3417/10/21/7548/s1>.

Author Contributions: Conceptualization, A.F., T.R.D., T.V.C., S.S., and T.S.; methodology, A.F., T.D., T.L., S.S., and E.C.L.B.; antimicrobial characterization: M.B., A.F., and D.J.; writing—Original draft preparation, all authors. All authors have read and agreed to the published version of the manuscript.

Funding: This research received no external funding.

Conflicts of Interest: The authors declare no conflict of interest.

References

1. Dhivya, S.; Padma, V.V.; Santhini, E. Wound dressings—A review. *BioMedicine* **2015**, *5*, 22. [CrossRef] [PubMed]
2. Xhaufaire-Uhoda, E.; Paquet, P.; Piérard, G.E. Dew point effect of cooled hydrogel pads on human stratum corneum biosurface. *Dermatology* **2007**, *216*, 37–39. [CrossRef] [PubMed]
3. Zidan, G.; Rupenthal, I.D.; Greene, C.; Seyfoddin, A. Medicated ocular bandages and corneal health: Potential excipients and active pharmaceutical ingredients. *Pharm. Dev. Technol.* **2018**, *23*, 255–260. [CrossRef] [PubMed]
4. Airiani, S.; Braunstein, R.E.; Kazim, M.; Schrier, A.; Auran, J.D.; Srinivasan, B.D. Tegaderm Transparent Dressing (3M) for the Treatment of Chronic Exposure Keratopathy. *Ophthalmic Plast. Reconstr. Surg.* **2003**, *19*, 75–76. [CrossRef]
5. Hunter, A.M.; Grigson, C.; Wade, A. Influence of topically applied menthol cooling gel on soft tissue thermodynamics and arterial and cutaneous blood flow at rest. *Int. J. Sports Phys. Ther.* **2018**, *13*, 483–492. [CrossRef] [PubMed]
6. Negut, I.; Grumezescu, V.; Grumezescu, A. Treatment Strategies for Infected Wounds. *Molecules* **2018**, *23*, 2392. [CrossRef]
7. Okur, M.E.; Karantas, I.D.; Şenyiğit, Z.; Üstündağ Okur, N.; Siafaka, P.I. Recent trends on wound management: New therapeutic choices based on polymeric carriers. *Asian J. Pharm. Sci.* **2020**, in press. [CrossRef]
8. Mi, F.-L.; Shyu, S.-S.; Wu, Y.-B.; Lee, S.-T.; Shyong, J.-Y.; Huang, R.-N. Fabrication and characterization of a sponge-like asymmetric chitosan membrane as a wound dressing. *Biomaterials* **2001**, *22*, 165–173. [CrossRef]
9. Ishihara, M.; Nakanishi, K.; Ono, K.; Sato, M.; Kikuchi, M.; Saito, Y.; Yura, H.; Matsui, T.; Hattori, H.; Uenoyama, M.; et al. Photocrosslinkable chitosan as a dressing for wound occlusion and accelerator in healing process. *Biomaterials* **2002**, *23*, 833–840. [CrossRef]

10. Ong, S.-Y.; Wu, J.; Mochhala, S.M.; Tan, M.-H.; Lu, J. Development of a chitosan-based wound dressing with improved hemostatic and antimicrobial properties. *Biomaterials* **2008**, *29*, 4323–4332. [[CrossRef](#)]
11. Hashimoto, T.; Suzuki, Y.; Tanihara, M.; Kakimaru, Y.; Suzuki, K. Development of alginate wound dressings linked with hybrid peptides derived from laminin and elastin. *Biomaterials* **2004**, *25*, 1407–1414. [[CrossRef](#)] [[PubMed](#)]
12. Trial, C.; Darbas, H.; Lavigne, J.-P.; Sotto, A.; Simoneau, G.; Tillet, Y.; Toët, L. Assessment of the antimicrobial effectiveness of a new silver alginate wound dressing: A RCT. *J. Wound Care* **2010**, *19*, 20–26. [[CrossRef](#)]
13. Maneerung, T.; Tokura, S.; Rujiravanit, R. Impregnation of silver nanoparticles into bacterial cellulose for antimicrobial wound dressing. *Carbohydr. Polym.* **2008**, *72*, 43–51. [[CrossRef](#)]
14. Forget, A.; Christensen, J.; Ludeke, S.; Kohler, E.; Tobias, S.; Matloubi, M.; Thomann, R.; Shastri, V.P. Polysaccharide hydrogels with tunable stiffness and provasculogenic properties via—helix to—sheet switch in secondary structure. *Proc. Natl. Acad. Sci. USA* **2013**, *110*, 12887–12892. [[CrossRef](#)]
15. Fernández-Cossío, S.; León-Mateos, A.; Sampedro, F.G.; Oreja, M.T.C. Biocompatibility of agarose gel as a dermal filler: Histologic evaluation of subcutaneous implants. *Plast. Reconstr. Surg.* **2007**, *120*, 1161–1169. [[CrossRef](#)] [[PubMed](#)]
16. Dumitriu, S. *Polysaccharides: Structural Diversity and Functional Versatility*, 2nd ed.; CRC Press: Boca Raton, FL, USA, 2004.
17. Forget, A.; Gianni-Barrera, R.; Uccelli, A.; Sarem, M.; Kohler, E.; Fogli, B.; Muraro, M.G.; Bichet, S.; Aumann, K.; Banfi, A.; et al. Mechanically Defined Microenvironment Promotes Stabilization of Microvasculature, Which Correlates with the Enrichment of a Novel Piezo-1 + Population of Circulating CD11b + /CD115 + Monocytes. *Adv. Mater.* **2019**, *31*, 1808050. [[CrossRef](#)]
18. Arnott, S.; Fulmer, A.; Scott, W.E.; Dea, I.C.; Moorhouse, R.; Rees, D.A. The agarose double helix and its function in agarose gel structure. *J. Mol. Biol.* **1974**, *90*, 269–284. [[CrossRef](#)]
19. Martin, B.C.; Minner, E.J.; Wiseman, S.L.; Klank, R.L.; Gilbert, R.J. Agarose and methylcellulose hydrogel blends for nerve regeneration applications. *J. Neural Eng.* **2008**, *5*, 221–231. [[CrossRef](#)] [[PubMed](#)]
20. Lyons, J.G.; Geever, L.M.; Nugent, M.J.D.; Kennedy, J.E.; Higginbotham, C.L. Development and characterisation of an agar-polyvinyl alcohol blend hydrogel. *J. Mech. Behav. Biomed. Mater.* **2009**, *2*, 485–493. [[CrossRef](#)] [[PubMed](#)]
21. Kajjari, P.B.; Manjeshwar, L.S.; Aminabhavi, T.M. Semi-interpenetrating polymer network hydrogel blend microspheres of gelatin and hydroxyethyl cellulose for controlled release of theophylline. *Ind. Eng. Chem. Res.* **2011**, *50*, 7833–7840. [[CrossRef](#)]
22. Rüther, A.; Forget, A.; Roy, A.; Carballo, C.; Mießmer, F.; Dukor, R.K.; Nafie, L.A.; Johannessen, C.; Shastri, V.P.; Ludeke, S. Unravelling a Direct Role for Polysaccharide β -Strands in the Higher Order Structure of Physical Hydrogels. *Angew. Chemie Int. Ed.* **2017**, *56*, 4603–4607. [[CrossRef](#)]
23. Forget, A.; Arya, N.; Randriantsilefisoa, R.; Miessmer, F.; Buck, M.; Ahmadi, V.; Jonas, D.; Blencowe, A.; Shastri, V.P. Nonwoven Carboxylated Agarose-Based Fiber Meshes with Antimicrobial Properties. *Biomacromolecules* **2016**, *17*, 4021–4026. [[CrossRef](#)] [[PubMed](#)]
24. Pluen, A.; Netti, P.A.; Jain, R.K.; Berk, D.A. Diffusion of macromolecules in agarose gels: Comparison of linear and globular configurations. *Biophys. J.* **1999**, *77*, 542–552. [[CrossRef](#)]
25. Arda, E.; Kara, S.; Mergen, Ö.B.; Pekcan, Ö. A comparison of fluorescence and UV-visible spectrometry techniques for thermal phase transitions of agarose gels. *Polym. Bull.* **2014**, *72*, 157–175. [[CrossRef](#)]
26. Forget, A.; Pique, R.-A.; Ahmadi, V.; Ludeke, S.; Shastri, V.P. Mechanically Tailored Agarose Hydrogels through Molecular Alloying with β -Sheet Polysaccharides. *Macromol. Rapid Commun.* **2015**, *36*, 196–203. [[CrossRef](#)]
27. Musolino, N.; Trout, B.L. Insight into the molecular mechanism of water evaporation via the finite temperature string method. *J. Chem. Phys.* **2013**, *138*, 1–17. [[CrossRef](#)]

28. Cesaretti, A.; Carlotti, B.; Gentili, P.L.; Clementi, C.; Germani, R.; Elisei, F. Spectroscopic investigation of the pH controlled inclusion of doxycycline and oxytetracycline antibiotics in cationic micelles and their magnesium driven release. *J. Phys. Chem. B* **2014**, *118*, 8601–8613. [[CrossRef](#)] [[PubMed](#)]

Publisher's Note: MDPI stays neutral with regard to jurisdictional claims in published maps and institutional affiliations.



© 2020 by the authors. Licensee MDPI, Basel, Switzerland. This article is an open access article distributed under the terms and conditions of the Creative Commons Attribution (CC BY) license (<http://creativecommons.org/licenses/by/4.0/>).